INVESTIGATION OF THE REACTOR CAVITY COOLING SYSTEM

EXPERIMENTAL FACILITY WITH RELAP5/SCDAPSIM SYSTEM CODE

A Thesis

by

MUSTAFA PEHLIVAN

Submitted to the Graduate and Professional School of
Texas A&M University
in partial fulfillment of the requirements for the degree of

MASTER OF SCIENCE

Chair of Committee,	Yassin A. Hassan
Committee Members,	Maria D. King
	Rodolfo Vaghetto
Head of Department,	Michael Nastasi

August 2021

Major Subject: Nuclear Engineering

ABSTRACT

The Reactor Cavity Cooling System (RCCS) is a passive safety system that is considered in the design of different advanced reactors. The RCCS operates during both normal and off-normal conditions as an important heat removal system. In this study, a RELAP5/SCDAPSIM system code model of the 1/23-scale water-cooled RCCS experimental facility at Texas A&M University has been generated and validated using experimental data from the facility under nominal conditions. The validated model was utilized to predict the thermal-hydraulic response of the RCCS under different operating conditions, including off-normal and accident scenarios. The comparison of the selected simulation results with the available experimental data confirmed the ability of the code to predict the behavior of the RCCS under the conditions analyzed.

DEDICATION

To my family, for their ever-present love and support.

ACKNOWLEDGEMENTS

CONTRIBUTORS AND FUNDING SOURCES

TABLE OF CONTENTS

LIST OF FIGURES

LIST OF TABLES

1. INTRODUCTION

Since the world expands sharply industrialized, energy demand in different and environment friendly energy sources, such as wind turbines, coal gasification and nuclear power has been increased. Since the origin of nuclear power on an industrial scale in the mid-20th century, fundamental reactor designs have progressed to maximize the six key factor attributes through the previous models [1].

The first attribute is cost-effectiveness. Nuclear power generation has become economically competitive compared to all other energy sources. The second one is safety. Through new reactor designs, safety is always the main concern and passive systems have more incorporation rather than active systems. The third one is security and nonproliferation. Minimizing the concern on risks of nuclear theft and terrorism all over the world is an important key factor for peaceful world. The fourth one is grid appropriateness. It is highly important to maintain the capability of local and national electric grid match, so to direct electric power. The fifth one is commercialization roadmap, which must include a logical timeline for reactor deployment. The sixth one is fuel cycle, which is critical in determining risk factors of nuclear safety, security and surety.

In the historical progress, four different reactor generations which are Generation I, II, III, and IV. Normally, Generation III is divided into two subcategories: Generation III and Generation III+, as it is shown in Figure 1.

1
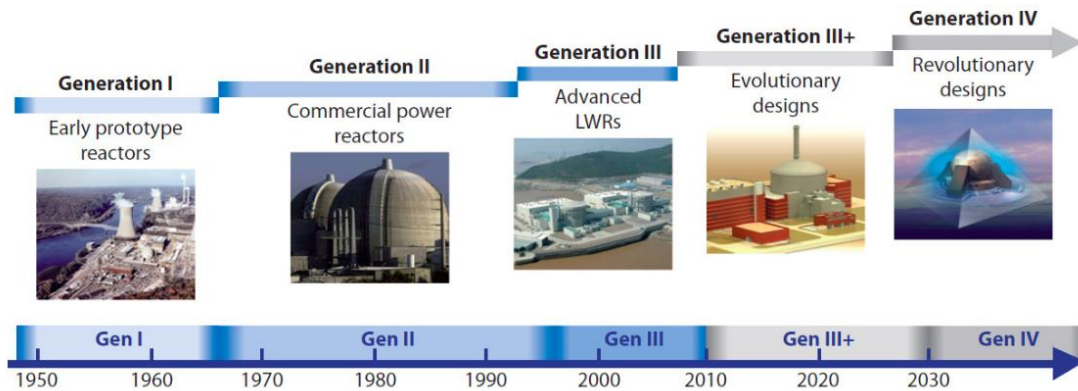
Figure 1. Generations of Nuclear Reactors. Reprinted from [2]

Gen I reactors refers to the prototype and the first civilian nuclear power plant from 1950s and 1960s. Gen II designs includes elements finalized to increase the safety and to reduce the risks associated with accidents. The most common Gen II reactors are water-cooled and moderated reactors (LWRs), advanced gas-cooled reactor (AGR), Canada deuterium uranium reactors (CANDU), and Vodo-Vodyanoi Energetichesky reactors (VVER). In Gen II reactors, the increasing in safety is achieved with active safety systems involving electrical or mechanical operations are embedded in the design. In an effort to advance safety, a new generation of advanced light-water reactors was designed in the mid-1990s. These Gen III designs incorporate so-called passive safety systems into the reactor structure to increase the reactor safety without any human intervention or electrical power. The Westinghouse 600MW advanced pressurized water reactor (PWR) AP-600 is an example for Gen III reactor. Develops based on Gen III reactors, Gen III+ reactor designs offer significant improvements in safety features. The most important improvement is the adoption of a specific type of passive safety, called

passive cooling. It is independent by any controls and relies on gravity or natural convection to control the off-normal conditions.

Gen IV nuclear plants designs, are designed to be highly economical, enhanced safety, producing minimal waste and being proliferation resistant. Gas-cooled fast reactors, molten salt reactor, lead-cooled fast reactors, supercritical-water-cooled reactor, sodium-cooled fast reactors, and very-high temperature reactor (VHTR) are six designs of Gen IV nuclear reactors.

From the Gen IV designs, very-high temperature reactor (VHTR), or high temperature gas-cooled reactor (HTGR), is a graphite-moderated, helium-cooled reactor with thermal neutron spectrum. It can supply nuclear heat over a range or core outlet temperatures between 700°C and 900°C, and potentially more than 1000°C in the future. Regarding to safety, in the HTGRs, passive safety systems that ensure the system in safe under off-normal (emergency or accident) conditions. Reactor cavity cooling system (RCCS) is the example that has been incorporated into the HTGR design.

Two different types of RCCS designs which are water-cooled RCCS and air-cooled RCCS are being considered and are of particular interest. The RCCS consists of a series of cooling panels located inside the reactor cavity and facing reactor pressure vessel (RPV), which provide the ability to passively remove the heat leaked from the RPV wall. The heat is transferred by radiation and convection to the RCCS panels, and then to the coolant (either air or water) flowing within vertical risers, that through natural circulation, carries it toward the external environment (in case of air) or to a heat

removal system within water tanks in the case of water-cooled design heat removal system. Without the need for any operator intervention, the temperature of structures, cavity and core can be kept under acceptable design limit during both normal operation and accident conditions.

The air-cooled RCCS convection principle is shown in Figure 2. Based on its working principle, cold air enters the system, carries the heat coming from the reactor cavity, and through buoyancy forces carries it out and dumps it in a heat sink without pumps, valves, or active components.
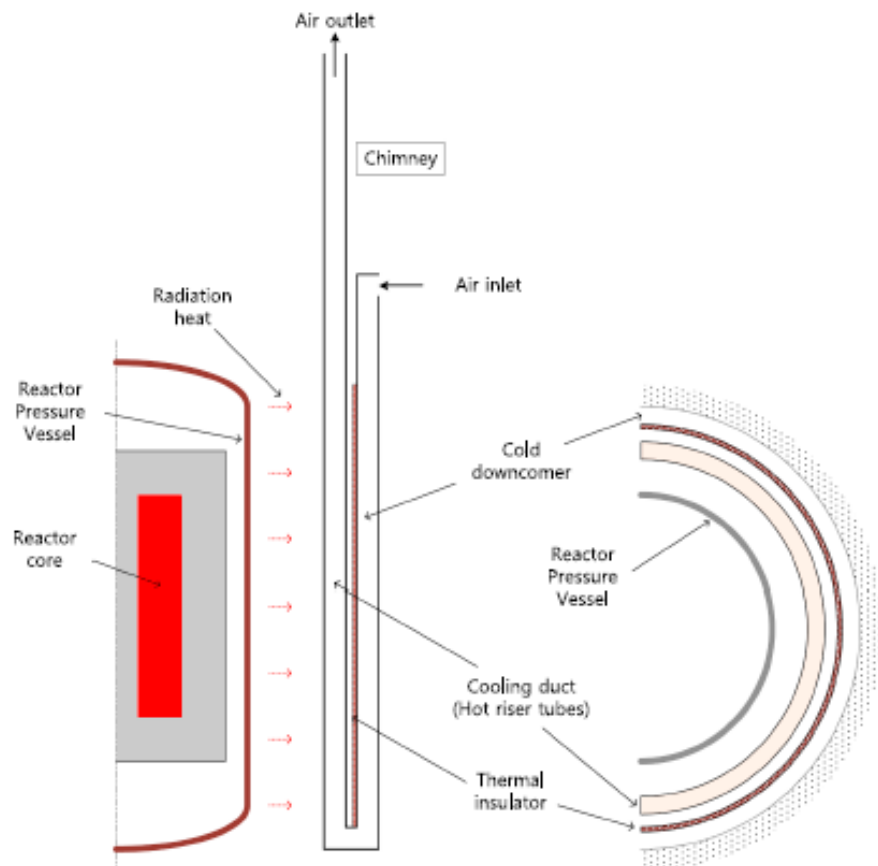
Figure 2. Air-cooled RCCS convection principle. Reprinted with permission from [3]

The basic water-cooled RCCS design is shown in Figure 3. Unlike the air-cooled RCCS, in the water-cooled RCCS, water is used to remove heat from the reactor cavity with natural circulation by buoyancy driven force. Cold water coming from the water tank reservoir reaches the cavity with cold leg. The temperature increase in water lets the water rising up through hot leg back to the water tank reservoir again. In the water tank, there is another system that cools down the temperature inside the reservoir, providing the ultimate heat sink that enables natural circulation. In normal operation conditions, the water remains subcooled. In case of off-normal conditions, the water reaches boiling after approximately 72 hours [1]. These RCCS designs are intended to remove heat from reactor cavity to keep safe both fuel and the cavity structures under design limits during normal operations and accident scenarios. The RCCS experimental facility at Texas A&M University was designed and built to study the thermal-hydraulic response of the RCCS during steady-state and transient conditions [4].
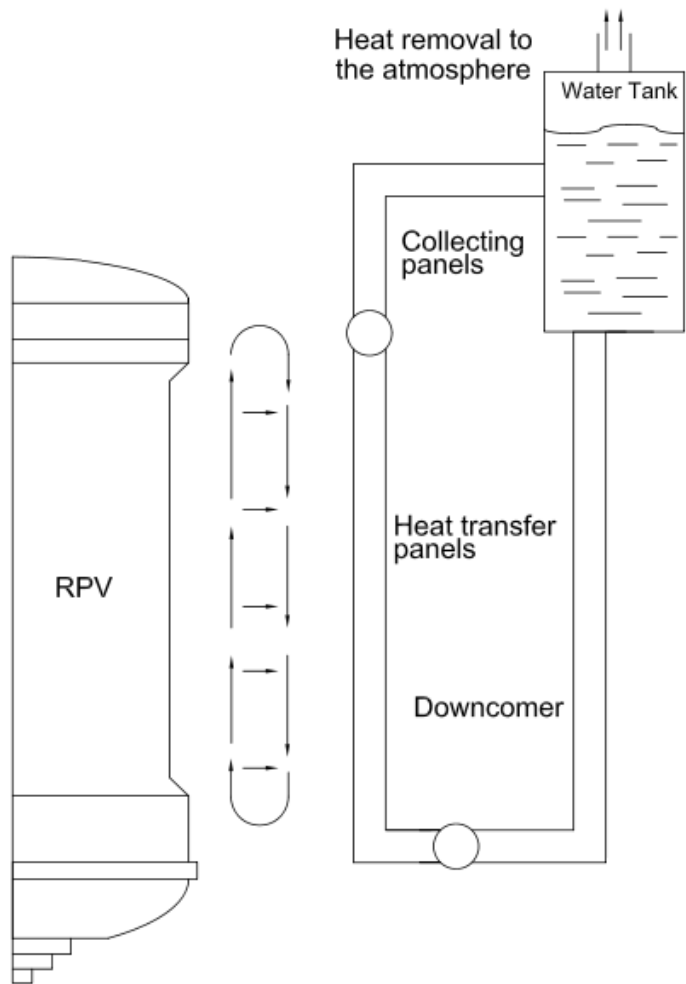
Figure 3. Water-cooled RCCS design overview. Reprinted with permission from [5]

2. OBJECTIVE OF THE THESIS

The proposed research aimed to:

I.   Investigate the flow split inside the risers region.

II. Analyze the stratification of the water inside the manifolds.

III. Investigate the effects of specific parameter (i.e., thermal power value) on the natural circulation inside the facility and on the overall response of the facility itself in relation of its main safety features.

IV. Predict the thermal hydraulic response of the facility under accident conditions that involve the loss of the active heat removal (two-phase, transient flow), identify the instabilities predicted by the model in relation to the instabilities published.

To achieve those goals:

a. A RELAP5/SCDAPSIM computational model of the TAMU water-cooled RCCS experimental facility under normal operation was prepared.

   a.1. The model was validated using the TAMU RCCS facility experimental data under steady-state condition

b. Through sensitivity analyses, the model described in point a is used to improve the comprehension of the facility response in relation to some of the important issues which had been identified in [6] (i.e. fouling and parallel channel interaction) and in relation to other phenomena.

3. LITERATURE REVIEW

The RCCS behavior has been studied in relation to many specific conditions [7]–[9]. The importance of the response of the RCCS under these conditions was highlighted for the first time in [10]. In the same study, more issues were evaluated and listed with:

- RCCS fouling on the coolant side
- Failure of one or more RCCS channels
- RCCS forced-to-natural circulation transition
- Single phase boiling
- Parallel channel interactions
- Natural circulation in a horizontal panel
- Vessel to RCCS effective view factors
- RCCS spatial heat loading

In [11], Quintanar et. al. studied the flow split (distribution) within a manifold with nine branches. In the conducted experiment, the system with the flow rate around 7.00 lpm goes under natural circulation and flow rate results behave similar differing in each riser.

Tompkins and Corradini in [12], and Lisowski et. al. in [13] studied the flow transition instabilities under accident condition that led to loss of coolant by evaporation, to analyze the two-phase natural circulation flow. In the experiment, the system undergoes a transition from laminar to two-phase flow regime.

Yan et. al. in [14] and Hou et. al. in [15] studied on six flow characteristics in two-phase natural circulation loop. Through their experimental research, they have found two flow modes, geysering and flashing, that are massively affecting the other flow modes. In the study, they also studied the power variations that are affecting the flow characteristics especially geysering and flashing.

In [16], Wang et. al. analyzed the nature of flashing-based natural circulation instability through four type of oscillations. They have found that with lower pressure and heat flux parameters, the natural circulation oscillations are being affected by flashing in excessively while in higher parameters, the flashing is suppressed.

Vaghetto et. al. in [17] analyzed the flow behavior through natural circulation under loss of active cooling system in the water tank. They have found different behaviors of flow which are symmetric distribution under subcooled and unstable, lower transition velocities, asymmetrical behavior under saturation conditions as the temperature increases in the system. The reason on different flow characteristics could be because of void fraction occurring at a different times and different values. Also, with the camera located at the upper manifold location, they have had a chance to record the flow inversion and stagnation during the saturation. Under this certain loss of active cooling system condition, the facility lasted more than 7.3 hours to maintain it's working in a proper way which is providing the cooling water to the heating panels and keeping the water temperature under the saturation temperature.

4. DESCRIPTION OF RCCS EXPERIMENTAL FACILITY

The water-cooled RCCS experimental facility at TAMU is a scaled (1:23) representation of a typical water-cooled RCCS design [18]. Figure 4 shows the facility in the Solidworks drawing and some of its details: The cooling panel with its nine risers inside the reactor cavity region, the lower and the upper manifolds binding the risers, the cylindrical water tank with its connecting pipes, and the chiller with its connecting pipes. The flow path is highlighted by red and blue arrows.

During the experiments resembling the RCCS normal operations, the heat is generated by three electrical radiant heaters, representing the RPV, and is transferred to the water inside the risers. To improve conduction between the risers, a thin metal panel (fins) that connects the risers was installed in the facility. The water temperature in the risers increases and the buoyancy forces allow the warmer water goes upward toward the top part of the facility. The water coming from the hot leg enters into the water tank where it is located at the top of the facility, mixes with cold water coming from the cooling system loop and returns back to the cooling panel through the cold leg. So, the natural circulation is ensured. All of the pipelines in the experimental facility were properly insulated to minimize heat losses. The water tank is open to the atmosphere to prevent pressurization of the system during tests.
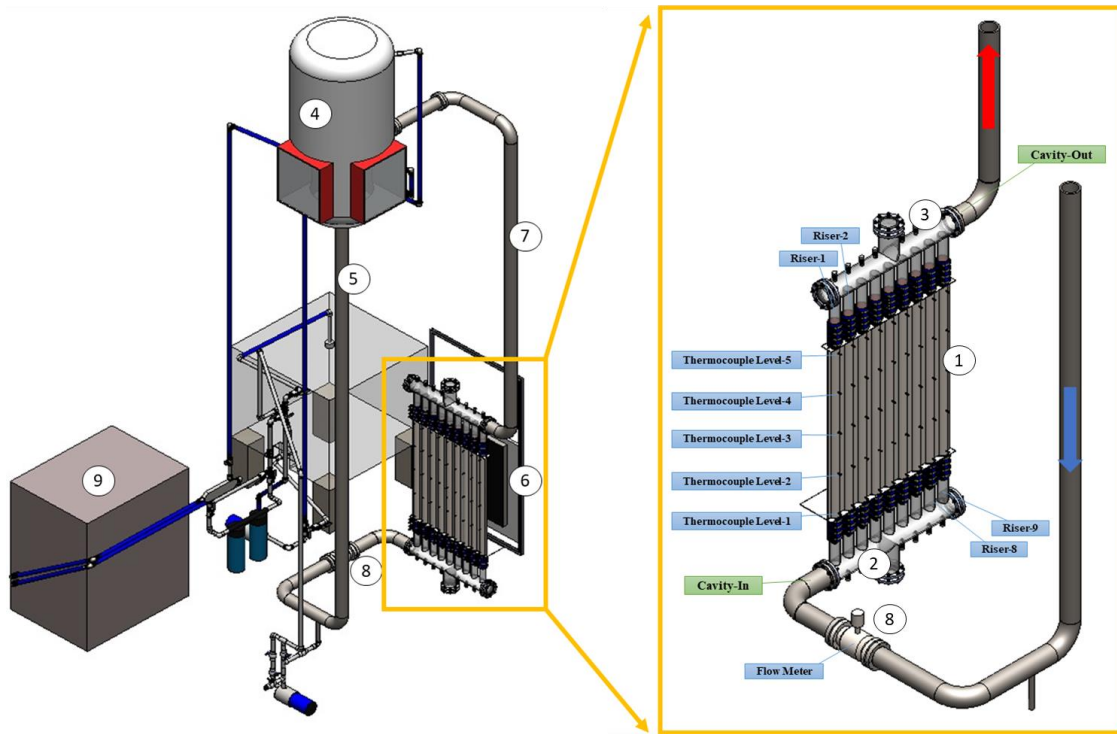
Figure 4. Solidworks Drawing of RCCS Experimental Facility (left) and zoomed in cavity section (right).

The facility is equipped with instrumentation to measure system level, thermal-hydraulic parameters such as flow rate, water temperatures etc. The flow meter was installed before the lower manifold and is able to record the total volumetric flow rate during the experiments. RTDs readings before the lower manifold and after the upper manifold are available. Thermocouples in the risers (five for each riser at different elevations) are used to record temperatures. Both flow meter and the thermocouple levels are highlighted with blue boxes in the right of the Figure 4. The pressure drop within the main loop can be controlled with a butterfly valve located at the bottom of the water tank, at the cold leg. The components that are labeled in the Solidworks drawing in Figure 4 are described and available in Table 1.

Table 1. Component description that are labeled in Figure 4.

Component #	Component Description	Dimension (m)	Orientation
1	Risers' Height	1.234	Vertical
2	Lower Manifold Flow Length	0.927	Horizontal
3	Upper Manifold Flow Length	0.927	Horizontal
4	Water Tank Height	1.676	Vertical
5	Cold Leg Flow Length	4.558	Vertical/Horizontal
6	Electrical Radiant Heaters	-	Vertical
7	Hot Leg Flow Length	3.187	Vertical/Horizontal
8	Flow Meter	-	-
9	Chiller	-	-

Experiments were performed at different valve opening to study the overall system response under different pressure drops within the primary loop. In this study, experimental data from tests conducted under two different valve opening setups (25% and 100%) were used to validate the prediction of the RELAP5/SCDAPSIM model. In Table 2, cavity in where it is at the entrance of the bottom manifold, cavity out where it is at the exit of the upper manifold temperature values and total system flow rate values for each case are tabulated with their fixed measurement uncertainty values. Cavity in and cavity out locations are shown in Figure 4.

Table 2. Experimental data from different pressure drop cases

Valve Opening Case (%)	System Flow Rate (lpm)	Temperature (°C)	
		Cavity In	Cavity Out
25	8.2 ± 0.3	35.8 ± 0.2	48.4 ± 0.2
100	39.0 ± 0.6	36.1 ± 0.2	38.9 ± 0.2

The axial temperature distribution of the cooling water within the nine risers of the panel are tabulated in Table 3 and Table 5 for both pressure drop cases. The temperatures are recorded using a set of forty-five thermocouples located at five different axial levels and each thermocouple's measurement uncertainty value is ± 1.1°K.

Table 3. The experimental data from a set of forty-five thermocouples for valve 25% open case

Part	Temperature (°K)				
	Level 1	Level 2	Level 3	Level 4	Level 5
Riser 1	308.81	308.95	312.75	316.35	320.55
Riser 2	308.69	308.81	312.95	316.35	320.05
Riser 3	308.98	309.03	313.15	316.55	319.95
Riser 4	308.84	308.88	312.95	316.55	319.85
Riser 5	308.83	308.84	313.05	316.75	320.25
Riser 6	308.77	308.87	312.75	316.35	320.05

Table 4. Table 3 Continued

Part	Temperature (°K)				
	Level 1	**Level 2**	**Level 3**	**Level 4**	**Level 5**
Riser 7	308.55	308.72	312.85	316.45	320.05
Riser 8	308.39	308.42	312.85	316.65	320.15
Riser 9	308.46	308.44	312.95	316.35	320.25

Table 5. The experimental data from a set of forty-five thermocouples for valve 100% open case

Part	Temperature (°K)				
	Level 1	**Level 2**	**Level 3**	**Level 4**	**Level 5**
Riser 1	309.25	309.35	309.25	311.05	312.75
Riser 2	309.15	309.25	309.35	310.25	311.85
Riser 3	309.35	309.35	309.45	310.25	311.65
Riser 4	309.25	309.25	309.35	310.15	311.45
Riser 5	309.25	309.25	309.45	310.05	311.55
Riser 6	309.25	309.35	309.25	309.45	310.95
Riser 7	309.15	309.15	309.25	309.45	310.35
Riser 8	309.05	308.95	309.25	309.55	310.15
Riser 9	309.15	309.05	309.35	309.35	309.75

5.   RELAP5/SCDAPSIM SYSTEM CODE AND MODEL PREPARATION

5.1. RELAP5/SCDAPSIM System Code

The RELAP5/SCDAPSIM is one of the thermal hydraulics analysis system code that is designed to predict the thermal hydraulic response of the reactor systems during normal operation and accident conditions. It is being developed as part of the international SCDAP Development and Training Program [19], [20]. The most advanced production version RELAP5/SCDAPSIM/MOD3.4 is production version of the RELAP5/SCDAPSIM and being used extensively in research reactors including TRIGAs, MTR-plate designs, nuclear power plant applications including Western designed PWRs and BWRs, Russian designed VVERs and RBMKs, Canadian and Indian designed CANDUs and HWRs, and Chinese designed PWRs. The code is also being used in general user training and for the design and analysis of severe accident related experiments. The RELAP5/SCDAPSIM/ MOD3.4 can also run a much spacious variety of transients including low pressure with the presence of non-condensable. Additionally, it can simulate not only all transients and postulated accidents but also severe accidents in the light-water reactor.

The code allows for simulations of equipment controllers, balance of plant equipment (turbine, accumulator, pipe). The code permits nodes to have not only geometry parameters (flow length, flow area) but also the initial condition parameters (temperature, pressure, even if the mass flow rate). With the time dependent volumes and time dependent junctions, boundary conditions can be set through system. User

defined working fluid, time and reference level (zero point) are available. Heat structure in model can be set based on their shape (cylindrical, spherical, and rectangular) and heat can be transferred to volumes by convection or radiation by defining heat structure either convection or radiation.

5.2. RELAP5/SCDAPSIM Nodalization Diagram

Based on the scaled experimental facility, a computational model is set up for RELAP5/SCDAPSIM to investigate not only the facility's response to steady-state conditions, but also its response to transitory conditions for scenarios that include transitioning to two-phase flow. Three simulation models were prepared for this study:

- The model for steady-state condition was prepared for validation the simulation results against the experimental data.
- The model for sensitivity studies was prepared to analyze flow split inside the risers region and investigate possible thermal stratification inside the manifolds and power reduction study.
- The model for hypothetical accident scenario including loss of active heat removal in the water tank was prepared to analyze flow characteristics under two-phase flow.

5.2.1. Nodalization Diagram for Steady-State Condition
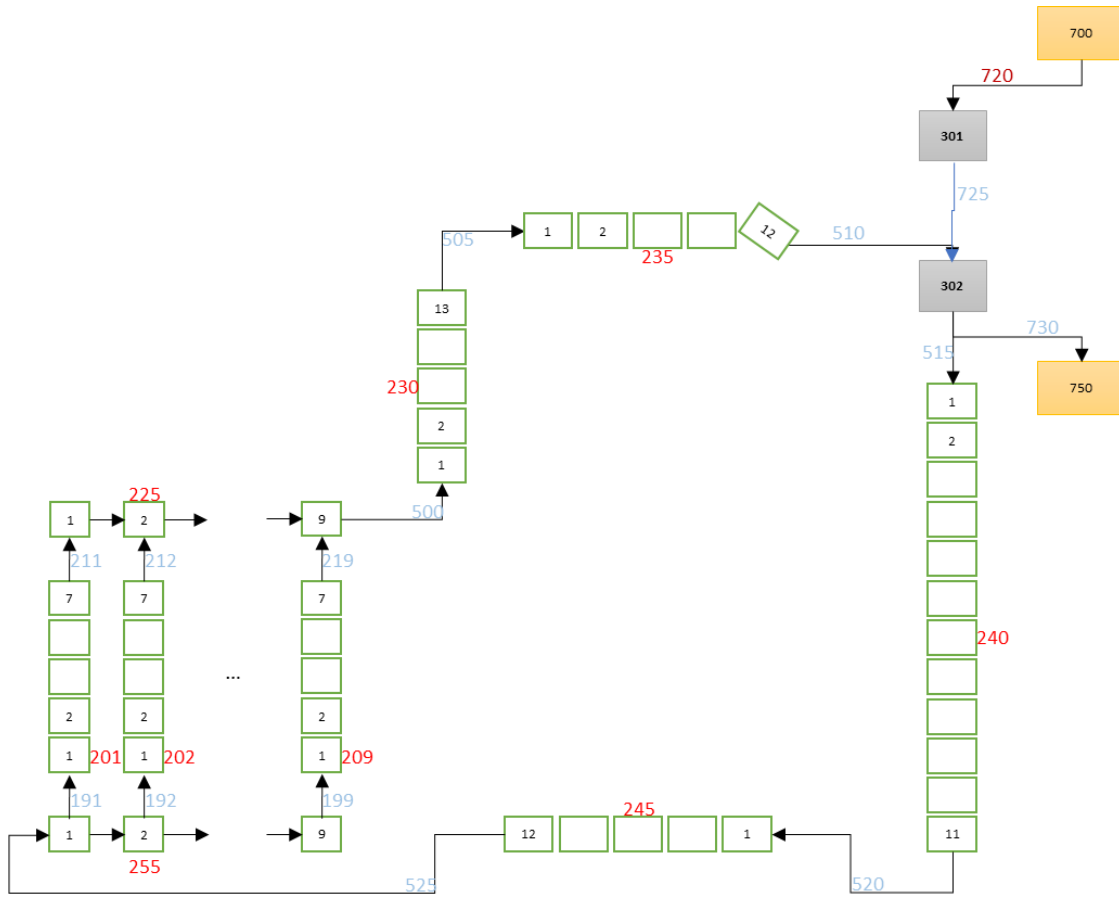
Figure 5. Nodalization diagram for steady-state condition (heat structures not shown)

The nodalization diagram for steady-state condition is shown in Figure 5. Two single volumes (301 and 302) represent the water tank. Figure 6shows how the water tank was modeled.
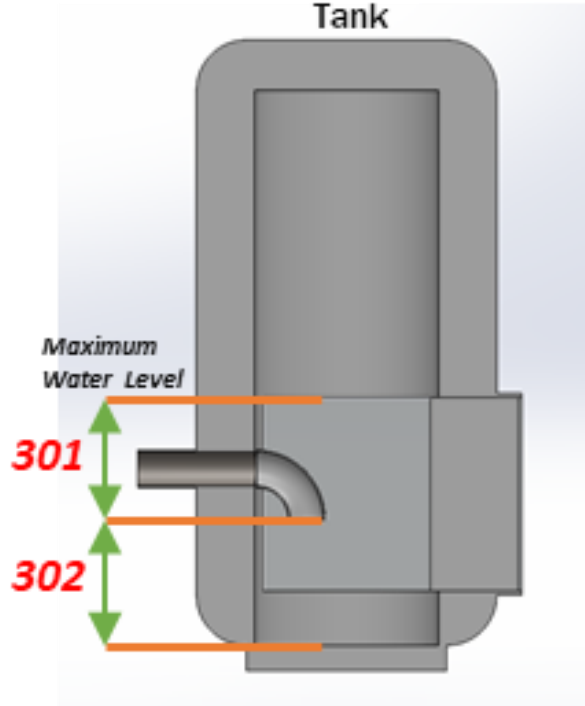
Figure 6. Modeling the water tank for steady-state condition simulation

The cold water flows down through the vertical section (component 240) and horizontal section (component 245) of the cold leg and enters the lower manifold (component 255) through the single junction 520, which is the part of the cavity. The lower manifold was modeled as a pipe with nine nodes, one for each riser, and connected with them through single junctions 191 throw 199. The vertical pipes 201 throw 209 represent the risers.
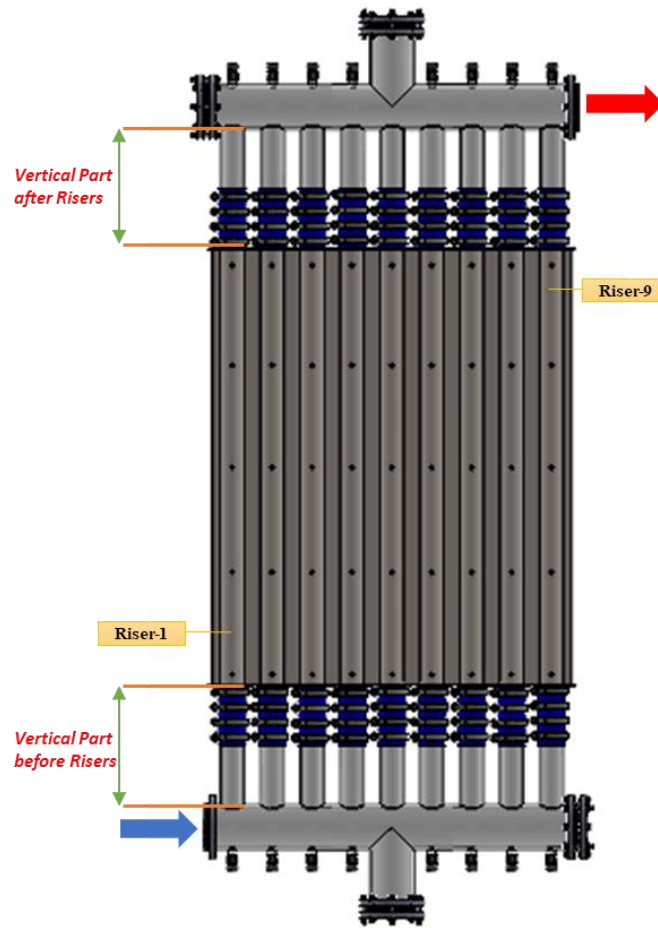
Figure 7. Experimental facility's cavity with vertical parts before and after risers.

Each riser was divided into seven nodes. The first and the last nodes represent the unheated vertical parts before the risers and after the risers through experimental illustration in Figure 7. The remaining five nodes (from second node to sixth node) are chosen so their center coincides with the thermocouple locations within each riser in the experimental facility. The heated water rises at the horizontal pipe with nine nodes (component 225), which represents the upper manifold. The hot water exits from the cavity and rises up until be discharged to the water tank through the vertical section (component 230) and horizontal section (component 235) of the hot leg in the model.

The elbow that is located inside the water tank that is shown in Figure 8 was modeled as well as a -45° inclined single volume (component 235-12 in Figure 5).
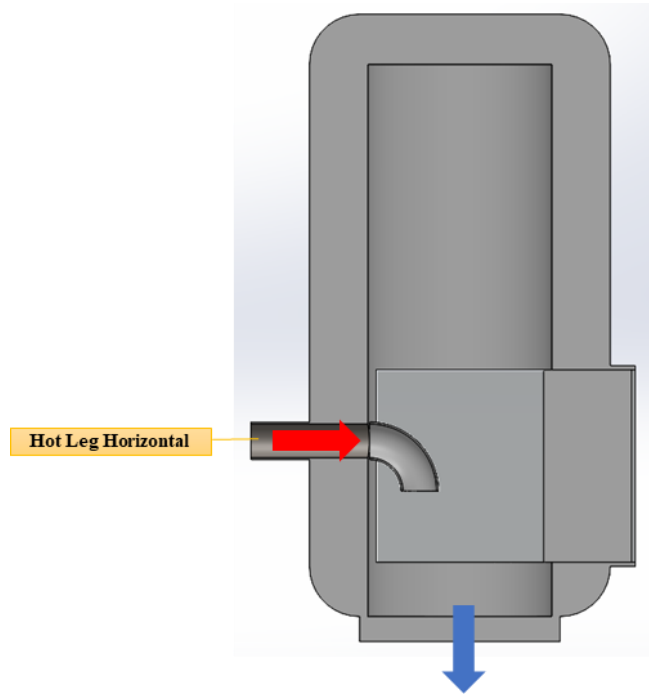
Figure 8. Modeling the elbow inside the water tank

For the boundary condition, two-time dependent volumes (700 and 750), one-time dependent junction (720), and one single junction (730) represent the chiller of the experimental facility are used. The pressure on top of 301 was set atmospheric pressure.

The RELAP5/SCDAPSIM allows to define heat structure with radiation and convection. In this study, the convection heat transfer was defined in the heat structure in the input file. The heat provided to the heat structure was split axially and lengthways in a manner that allow the simulations to match the temperature differences recorded by the thermocouples during the experiments. Given that the experimental temperature measured by the lowest level of thermocouples inside the risers is lower than the

experimental temperature measured at the cavity inlet, a heat loss was imposed in the lower part of the risers (first node). The power calculations to determine the net power inside the risers region in relation to experimental data was made with using Eq (*1*. So, that power led to assign computational heat source and heat loss values.

$$\text{Power} = \dot{m} * c_p * \Delta T \tag{1}$$

Where:

$\dot{m}$: mass flow rate (kg/s)

c_p : specific heat (J/kg*K)

ΔT : temperature difference (K)

The total system flow rate flowing through the cavity and the cavity in and cavity out temperatures for valve 25% open and valve 100% open cases from experimental data are tabulated in Table 6.

5.2.2. Nodalization Diagram for Sensitivity Studies

In addition to the steady-state condition model, a new model was created to simulate more in detail the manifolds and investigate possible stratification. Thus, the lower and upper manifolds were divided into three pipes as shown in Figure 9. Single junctions were added to connect each of the nodes to its upper and lower neighbors through.

To explain the results easily, the upper manifold pipe components 225, 226 and 227 are being represented by upper manifold bottom, middle and top components respectively.
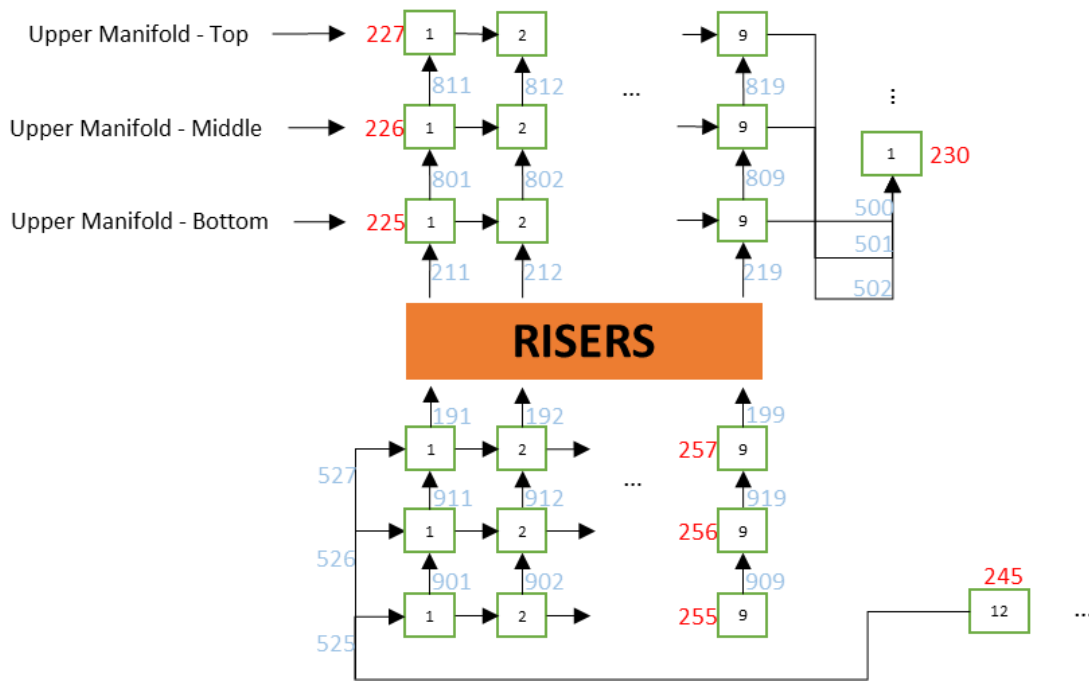
Figure 9. Cavity section's nodalization diagram for stratification sensitivity study.

5.2.3. Nodalization Diagram for Two-phase Flow Analysis

For the two-phase flow analysis, the steady-state condition model was upgraded with the water tank nodalization as shown in Figure 11. In the new model the water tank was divided into three single volumes and the Solidworks drawing in Figure 10 shows how the single volumes are illustrated.
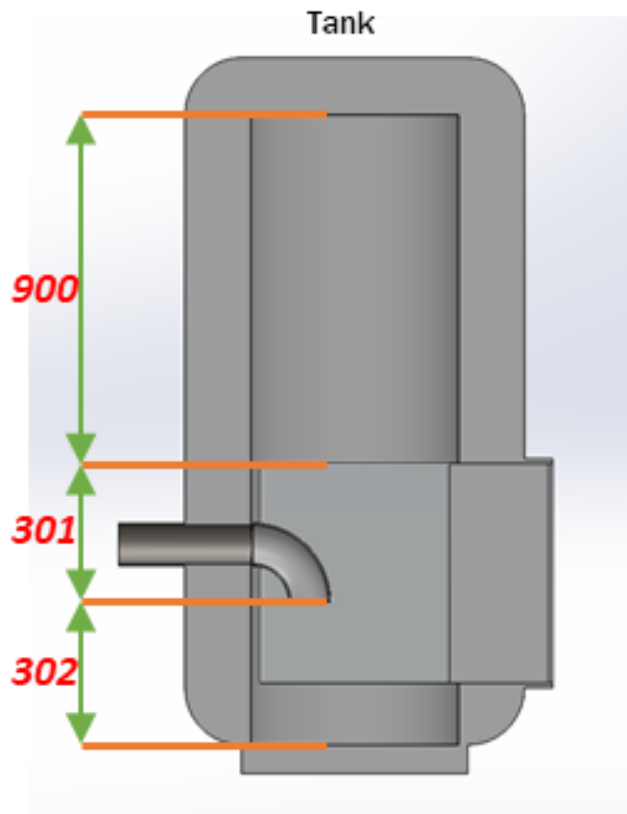
Figure 10. Water tank modeling for two-phase flow analysis.

The component 900 represents the top of the water tank which was modeled to allow the coolant to expand due to the transitory condition. The top of the water tank was kept at 1 atm pressure through the simulation duration. The nodalization approach on this two-phase flow analysis was explained in the following results and discussion section in corresponding sub section.
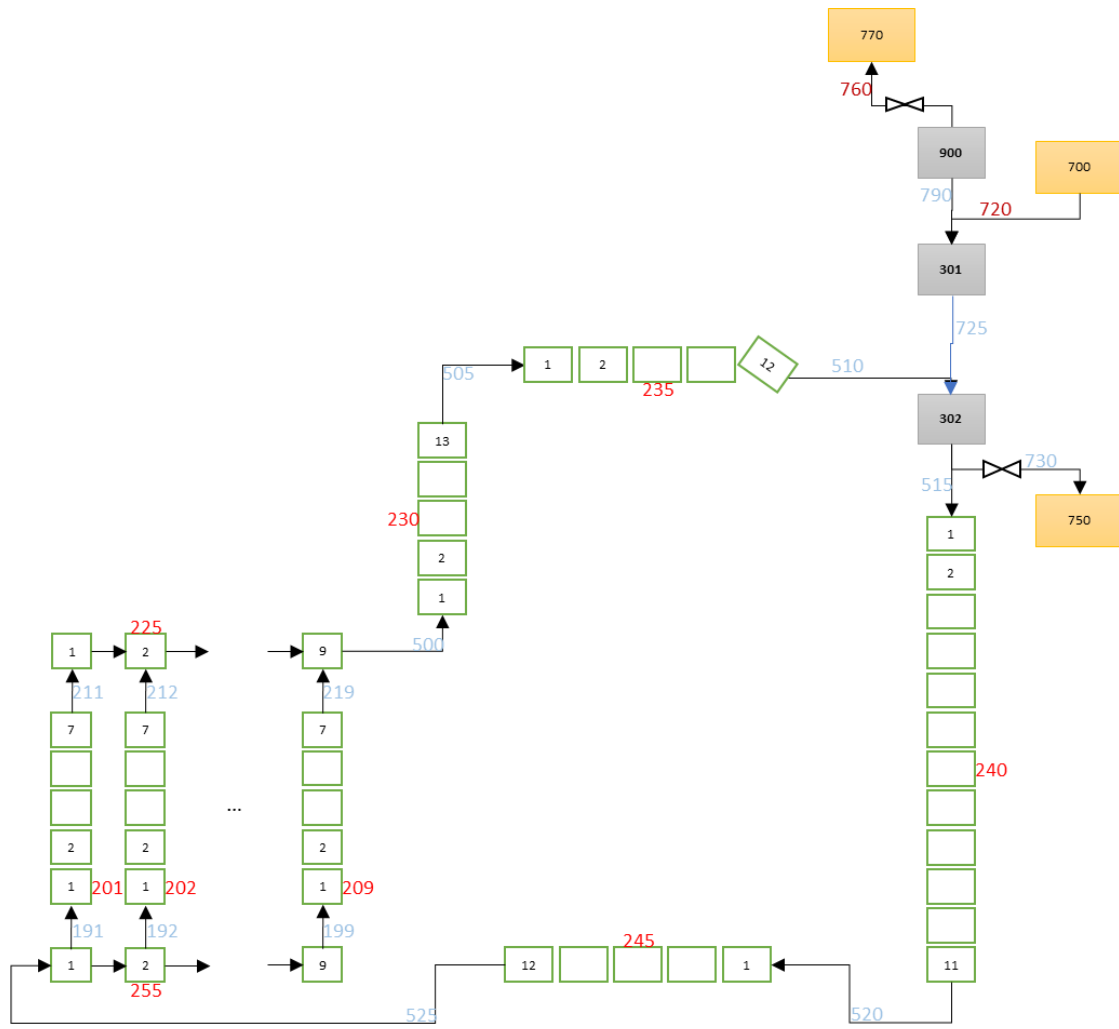
Figure 11. Nodalization diagram for two-phase flow analysis

6. RESULTS AND DISCUSSION

6.1. Steady-state Condition Model Results

Based on the phenomena on ensuring steady-state condition, temperature difference between cavity in and cavity out and the total system flow rate should be constant. In this study, the cases that are related to three different simulation models were investigated. With the steady-state condition model, the model results were tried to validate against experimental data. With the averaged the specific heat values for each case from the cavity in and cavity out temperature, the net power values were calculated for each case are reported in Table 6 below.

Table 6. Parameters for power calculation inside the cavity from experimental data

Valve Opening Case (%)	25	100
Volumetric Flow Rate (lpm)	8.2 ± 0.3	39.0 ± 0.6
Mass Flow Rate (kg/s)	0.1358 ± 0.005	0.6460 ± 0.01
Cavity In Temperature (°C)	35.8 ± 0.2	36.1 ± 0.2
Cavity Out Temperature (°C)	48.4 ± 0.2	38.9 ± 0.2
Net Power (W)	7153.12 ± 286.8[1]	7555.56 ± 551.4

Two different pressure drop cases were simulated. The starting point was from defining the heat source and heat loss distributions inside the risers in relation to the experimental data that received for valve 25% open case. This case was chosen because

---

[1] The error value was calculated with error propagation for multiplication formula.

the lower flowrate result in higher temperature jumps inside the risers, that – given the fixed 1.1 °C of error associated with the thermocouple measurements – reduces the relative error of the experimental data set used to tune the input parameters. Once completed, the pressure drop inside the loop was controlled with changing the flow area of the node in vertical section of the cold leg in corresponding location. With some iterations in the heat source, heat loss and friction loss in relation to flow area heat source and heat loss values that are shown in Table 7 were used.

Table 7. Heat source and heat loss values that are used in simulations

Valve Opening Case (%)	Heat Source (W)	Heat Loss (W)	Net Power (W)
25	7368.64	255.78	7112.86
100	7992.28	389.37	7602.91

The simulation results were analyzed in two different approach. The first one is about the temperature results from the thermocouple levels and the second one is from cavity in, cavity out temperature and the system flow rate values. The reason behind this was because of different measurement uncertainty values from experimental data. Also, the flowrate was converted from mass flow rate to volumetric flow rate with using basic density equation. In corresponding place that flow meter installed in the experimental facility, in the model the water density, mass flow rate in corresponding node were used to find total system flow rate. The simulation was cut after reaching and continuing in steady-state condition in not only system flow rate value but also the temperature results in the heating section.

Figure 12 shows the simulation temperature results inside each riser's thermocouple levels for valve 25% open case. The temperature range is from 309.0°K to averagely 320°K. and the temperature distribution in each riser is showing similar increasing trend.
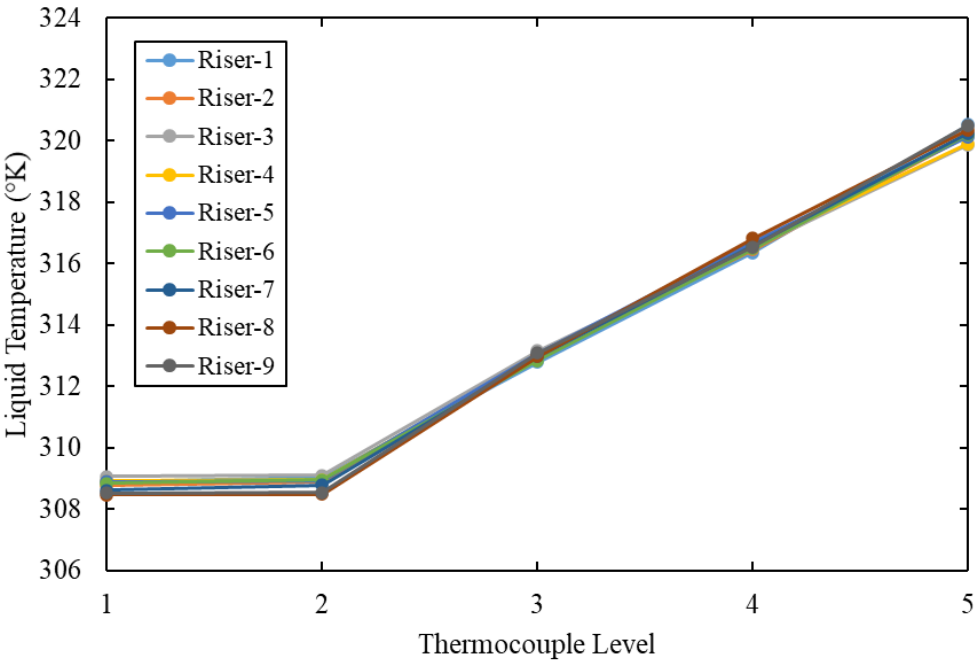
Figure 12. Simulation temperature results for valve 25% open case through each thermocouple level

When the simulation results were compared with the experimental data based on each thermocouple level temperature results, the results for both computational results and experimental data were overlapping in each location in Figure 13.

Figure 13. Simulation temperature results comparison with experimental data in order to first thermocouple level (a), second thermocouple level (b), third thermocouple level (c), fourth thermocouple level (d), fifth thermocouple level (e) for valve 25% open case. The error bar in each experimental data graph is ±1.1°K.

Also, the cavity in, cavity out and the total system flow rate results were compared with the experimental data in Table 8, the results were perfectly positioned inside the measurement uncertainty value that coming from the experimental data.

Table 8. Simulation results comparison with experimental data in order to total system flow rate, cavity in, and cavity out temperature values for valve 25% open case

	System Flow Rate (lpm)	Cavity In Temperature (°K)	Cavity Out Temperature (°K)
Experimental Data	8.2 ± 0.3	309.0 ± 0.2	321.6 ± 0.2
Simulation Results	8.15	309.07	321.67

After validation of the computational results for valve 25% open case against the experimental data, valve 100% open case was simulated. In this case, same heat distribution inside the risers' parameters was used but different corresponding heat source, heat loss and friction loss parameters in relation to the flow area shown in Table 7. Based on same way that was followed in the valve 25% open case, the Figure 14 illustrates the temperature results inside each riser's thermocouple level for valve 100% open case. Due to the heat distribution inside the cavity, the temperature results for riser 1 is the hottest and riser 9 is the coldest component. The development of the temperature inside the thermocouple level 1 and 2 are similar. After thermocouple level 3, temperatures are scattered.
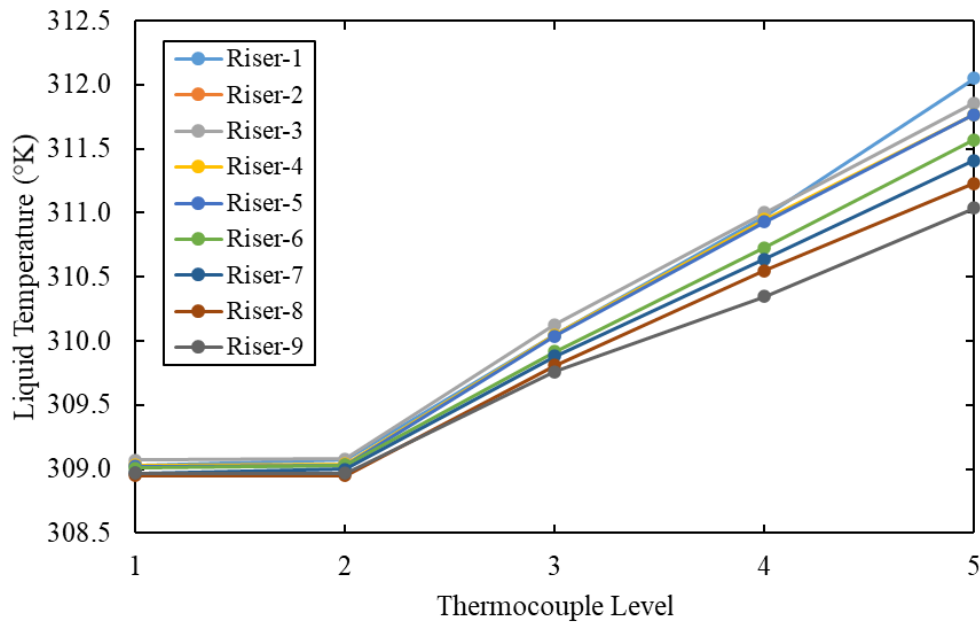
Figure 14. Simulation temperature results for valve 100% open case through each thermocouple level

In Figure 15, comparison between experimental data, while in the thermocouple levels 1 and 2 were showing the similar behavior and the temperature results were pretty much overlapping each other, in the thermocouple levels 3, 4 and 5 the computational temperature results were showing a trend that computational results were higher than the experimental data. The reason behind on the divergence in thermocouple level 3 to 5 could be happened because in the simulation, the cavity in and cavity out temperature values were tried to match first due to having lower fixed measurement uncertainty value than the thermocouple levels in the risers. Also, in the real experimental facility, the heat losses were distributed throughout the entire loop while in the simulation model, the heat losses were concentrated only in each riser's first node based on the experimental data that received.
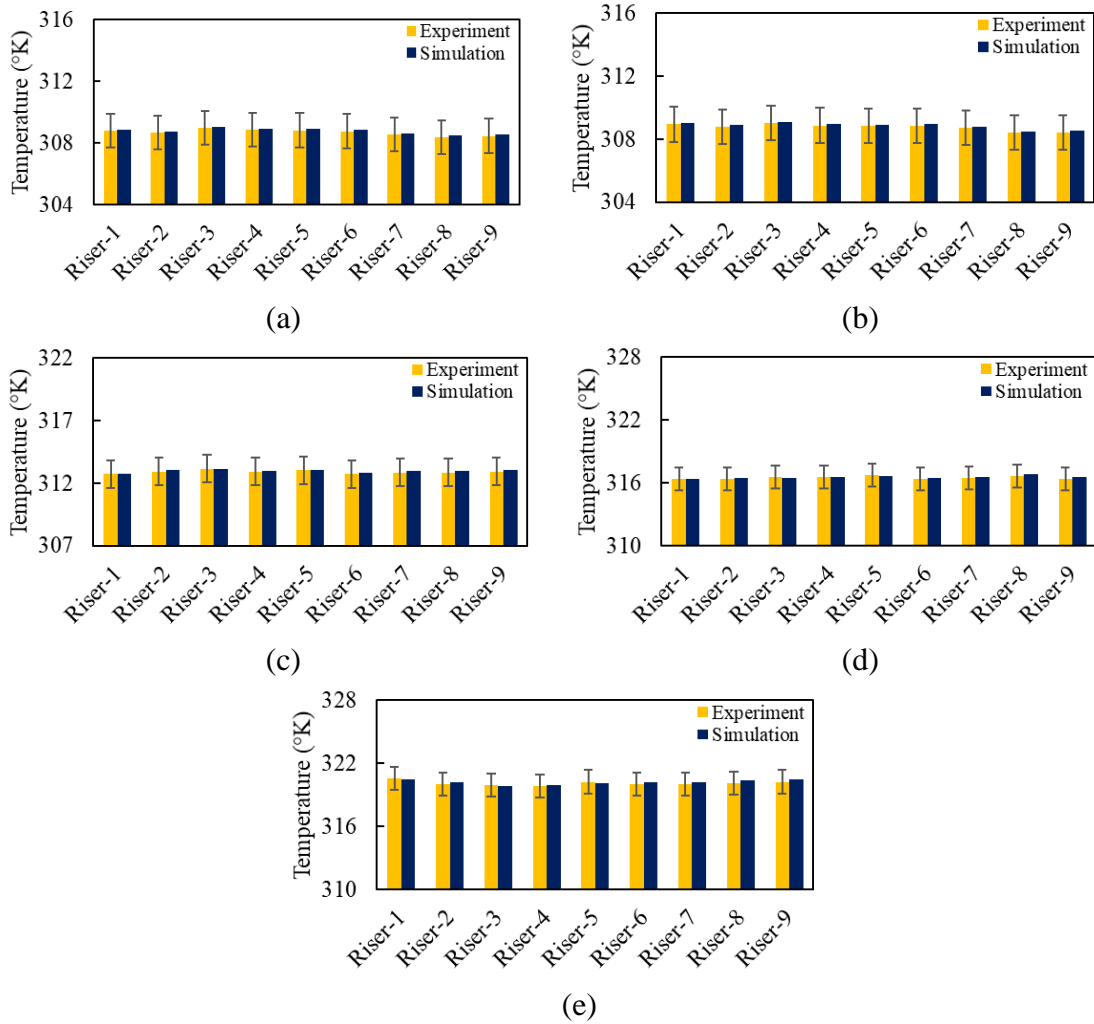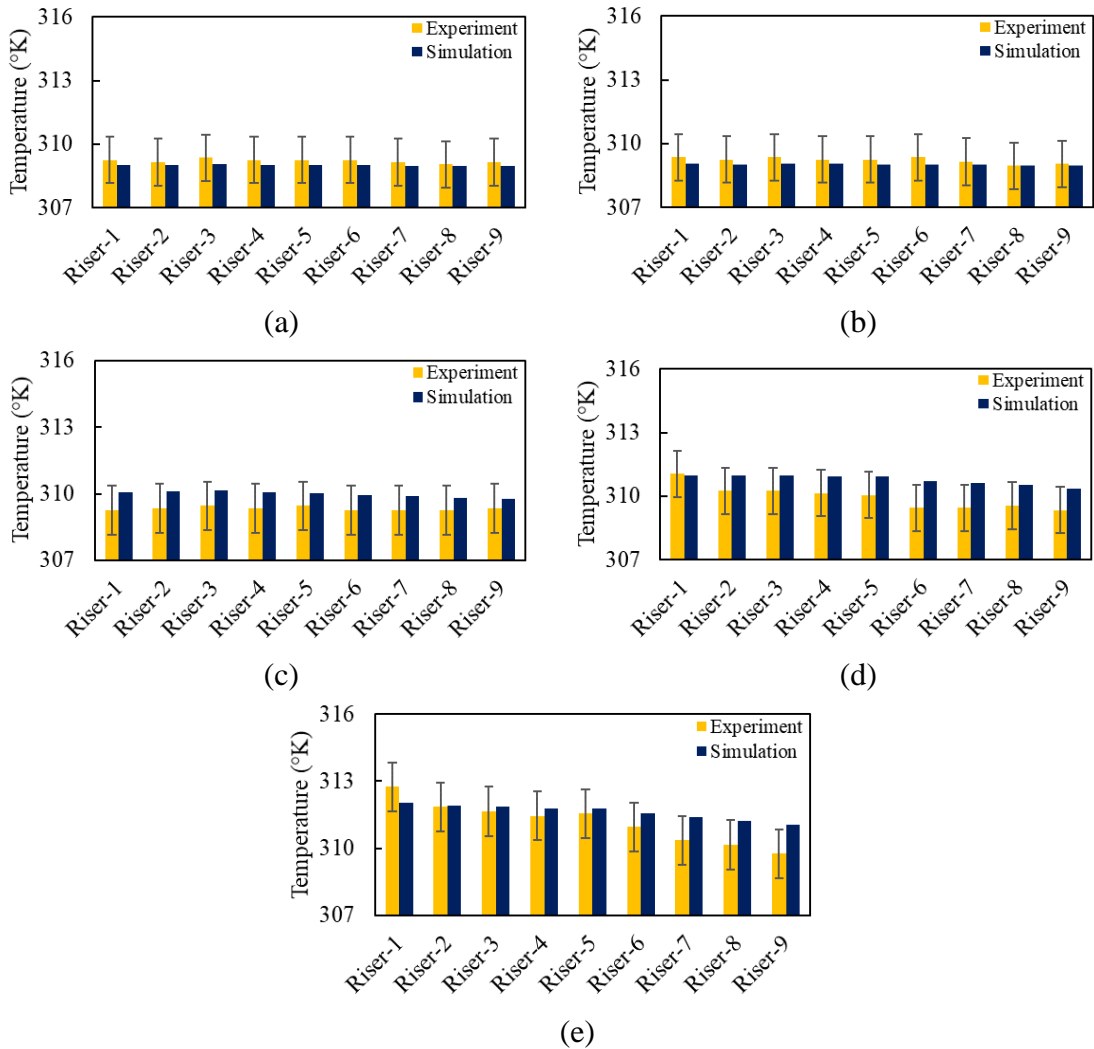
Figure 15. Simulation temperature results comparison with experimental data in order to first thermocouple level (a), second thermocouple level (b), third thermocouple level (c), fourth thermocouple level (d), fifth thermocouple level (e) for valve 100% open case. The error bar in each experimental data graph is ±1.1°K.

When the system flow rate, cavity in, and cavity out temperature results from simulations were compared with the experimental data, the results were still inside the measurement uncertainty range shown in Table 9. Based on the simulation results, RELAP5/SCDAPSIM model for steady-state condition has good agreement in both cases.

Table 9. Simulation results comparison with experimental data in order to total system flow rate, cavity in, and cavity out temperature values for valve 100% open case

	System Flow Rate (lpm)	Cavity In Temperature (°K)	Cavity Out Temperature (°K)
Experimental Data	39.0 ± 0.6	309.3 ± 0.2	312.1 ± 0.2
Simulation Results	39.06	309.11	311.92

6.2. Sensitivity Study Results from Flow Split in Each Riser

For the sensitivity analysis, the flow splits in each riser for both valve 25% open and valve 100% open cases were analyzed. In the Figure 16, values illustrate the flow rates in each riser for valve 25% open case. Riser 1 was located close to the cavity inlet while riser 9 was located close to cavity outlet. Based on the results, in the valve 25% open case, the flow distribution in each riser was between 0.0864 lpm to 0.953 lpm. Results demonstrated that the flow behaved similarly and distributed with difference almost 10% in maximum. According to the reference [11], experiments with the low volumetric flow rate showed similar behavior and results were showing good agreement.
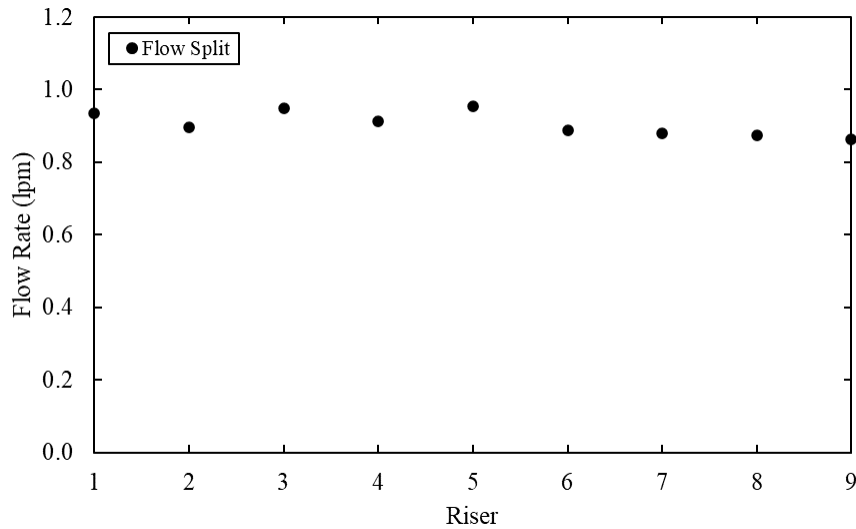
Figure 16. Volumetric flow split in each riser for valve 25% open case

When the results for valve 100% open case were analyzed in Figure 17, the flow splits behaved in a different way. The difference between the lowest and the highest flow rate was around 1.53lpm. The difference based on the temperature in riser 1 and riser 9 was quite a bit differed due to the heat distribution inside the risers. The temperature results in riser 1 were higher than in riser 9 and based on the phenomena that is lower temperature increasing with higher flow rate; the simulation temperature results were supporting the phenomena. So that explained why the flow splits were behaving in a different way from the valve 25% open case's flow split results.
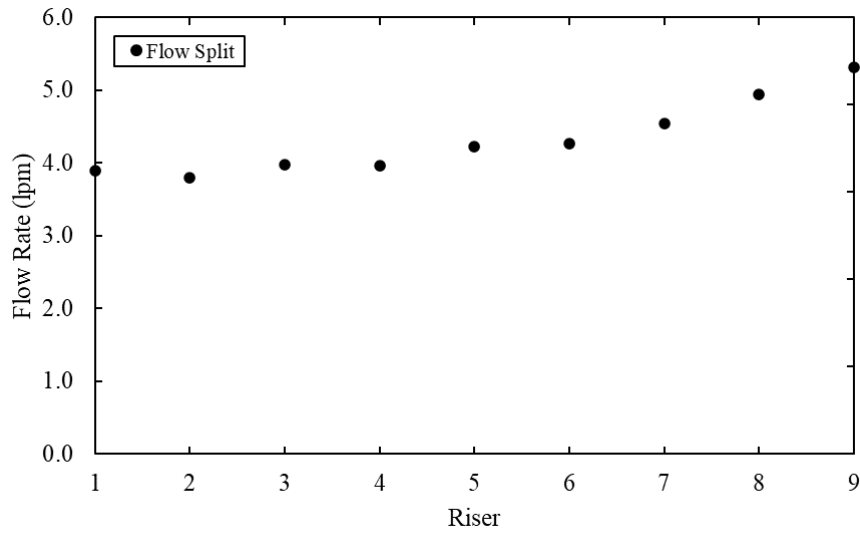
Figure 17. Volumetric flow split in each riser for valve 100% open case

The flow split results inside each riser are also tabulated and shown in Table 10.

Table 10. Volumetric flow split results for both pressure drop cases

Case \ Part	Flow Rate (lpm)	
	Valve 25% Open	Valve 100% Open
Riser-1	0.934	3.900
Riser-2	0.896	3.799
Riser-3	0.949	3.981
Riser-4	0.912	3.966
Riser-5	0.953	4.226
Riser-6	0.888	4.270
Riser-7	0.880	4.550
Riser-8	0.875	4.938
Riser-9	0.864	5.428

6.3. Sensitivity Study Results from Stratification in Manifolds

As the model's nodalization diagram described above, for another sensitivity analysis, the Figure 9 shows that the model with stratification in upper and lower manifolds. In the model, upper and lower manifold components were divided into 3 pipes with equal flow areas. With the single junctions, each node out of nine nodes in the components were connected in a relation to its lower and upper parts. The exit parts were connected into the hot leg vertical part in same location. The upper manifold components 225, 226 and 227 were being illustrated with upper manifold bottom, middle and top component respectively to explain the temperature distribution inside the manifold easily. Both valve 25% open and 100% open cases were simulated. The Figure 18 shows the temperature distribution results in each upper manifold components and riser's 7th node for valve 25% open case.
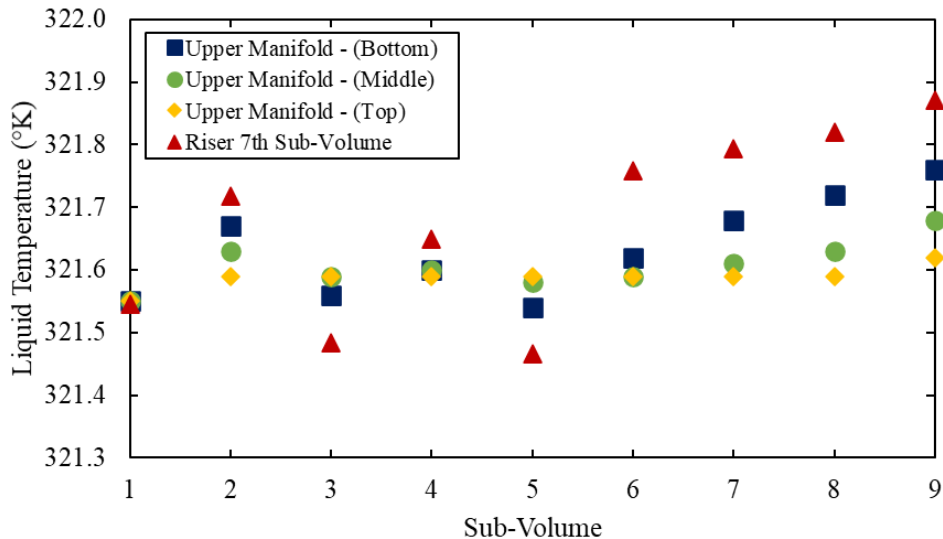
Figure 18. Water temperature distribution through stratification analysis in upper manifold for valve 25% open case.

When the results for valve 25% open case were analyzed in the upper manifold, the temperature distribution was differing between maximum 0.24°C. In the nodes between 1 to 5, results showed quite a bit oscillating behavior and from node 5 to 9 the results were differed from each other. The reason on this behavior was hot/cold water coming from each riser's 7th node was feeding the upper manifold bottom component's each node and those nodes were affecting their forward and above nodes. Because of flow continuing through simulation, the water condition coming from the riser's 7th node was determining the upper manifold's temperature distribution in each component.
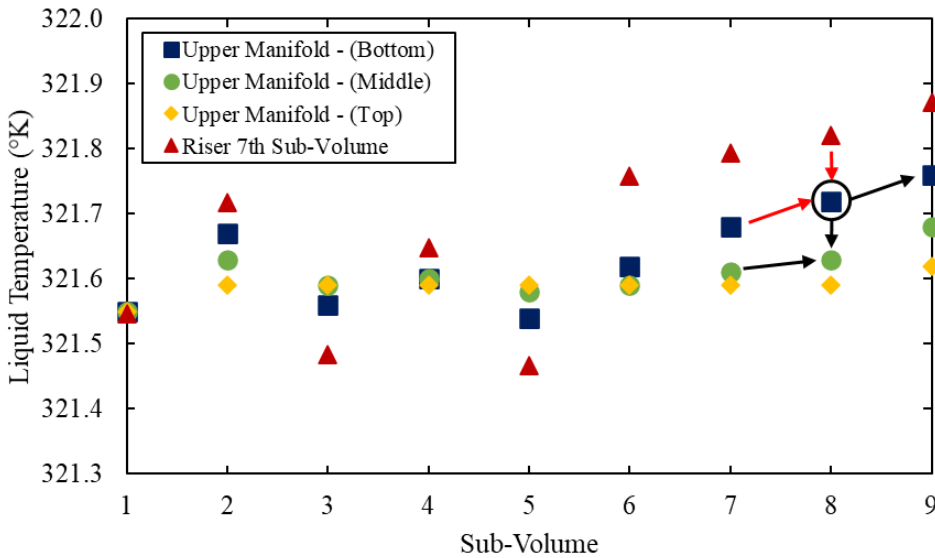
Figure 19. Water affecting ways with green shapes for stratification analysis

To explain in a different way, in Figure 19, water in the black circled node which is upper manifold bottom component's 8th node was being affected by riser 8's 7th node and was affecting both upper manifold bottom component's 9th node and upper manifold middle component's 8th node. And that condition applied to the other sub-volumes.

36

In the meantime, results for valve 100% open case were analyzed in a similar

approach that was followed in valve 25% open case. The temperature distribution was

differing approximately 0.6°C from upper manifold bottom to upper manifold top

components. The same idea about water coming from each riser's 7th node feeding the

upper manifold bottom component nodes that lined up with temperature distribution in

valve 25% open case results, the temperature distribution for valve 100% open case was

interpreted and shown in Figure 20.
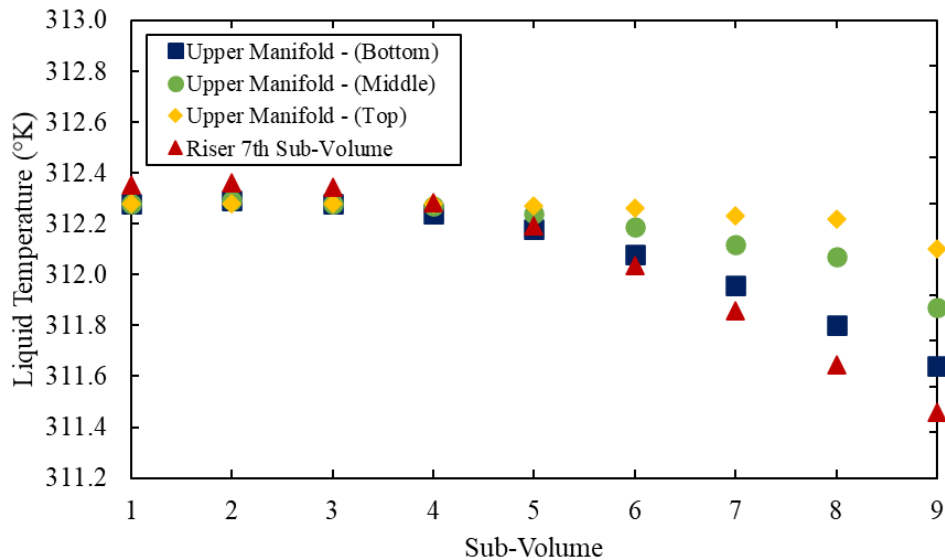
Figure 20. Water temperature distribution through stratification analysis in upper
manifold for valve 100% open case.

From the valve 100% open case's results, it is seen that water in upper manifold

top component is hotter than the water in upper manifold bottom component. Because

the water temperature in each riser's 7th node was showing gradually decreasing

behavior, the water temperature in upper manifold's bottom, middle and top components

were distributed as in the shown way.

Based on not seeing any difference in the lower manifold's stratification from the preliminary results, there was not focus on interpretation for it.

6.4. Sensitivity Study Results from Power Reduction

For another sensitivity analysis, the power reduction for valve 25% open case was investigated. With this study, it was aimed to investigate effects of power inside the risers to the temperature results and system flow rate without controlling the system flow rate from the butterfly valve. From that, the model for valve 25% open case was chosen. The reason behind that was because model's results for valve 25% open case was more accurate than the results from valve 100% open case. For the procedure, the power values were reduced by 10% and 20% and the model was simulated in steady-state condition. The temperature results according to the thermocouple levels are shown in the Figure 21.

(a)   (b)

(c)

(d)

(e)
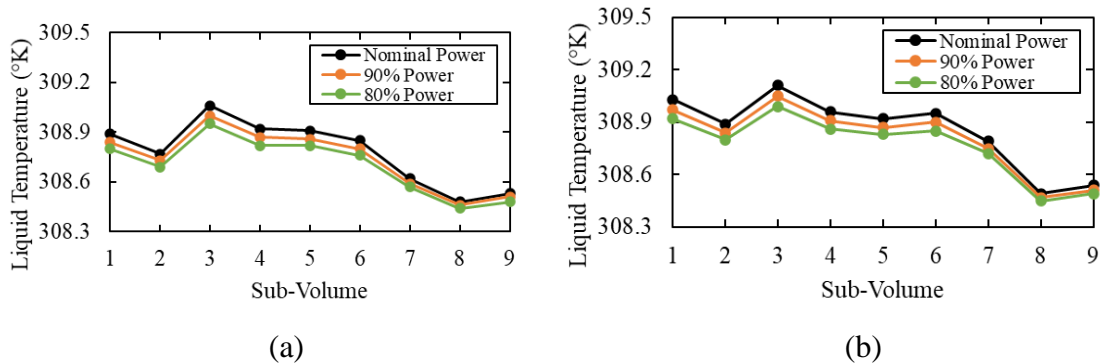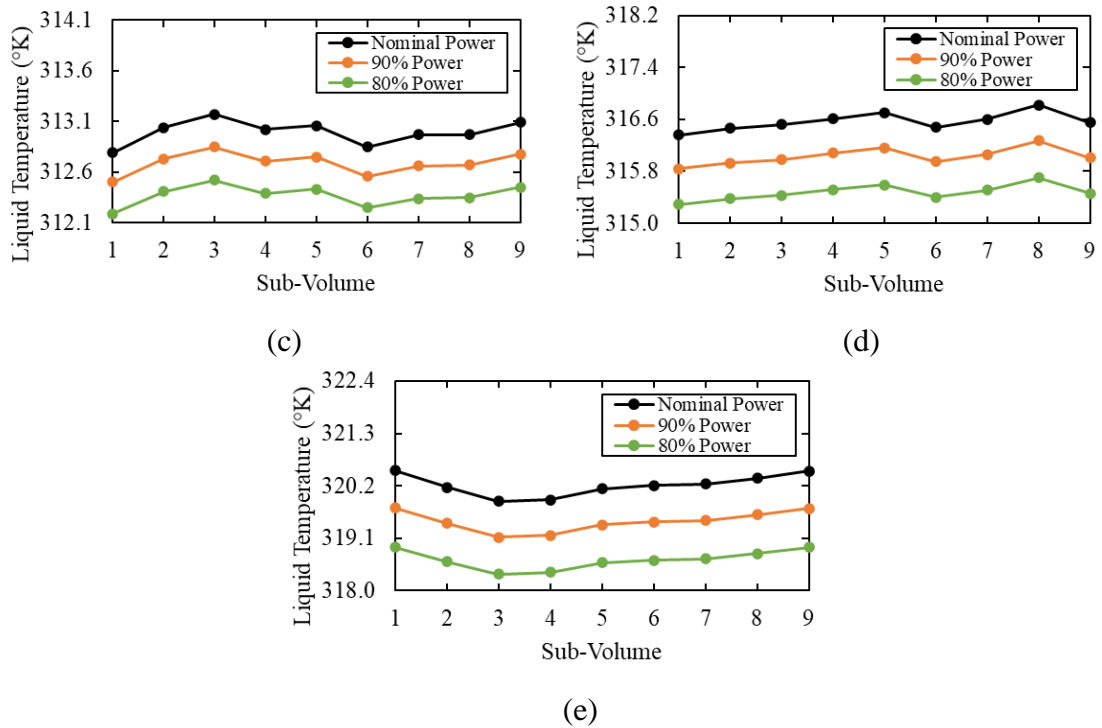
Figure 21. Temperature results from power reduction sensitivity analysis for valve 25% open case.

In the thermocouple 1 and thermocouple 2 levels, the temperature results were showing slightly separation from each other. That was not only because of the heat distribution in the thermocouple 1 and 2 areas but also because of the heat loss in each riser's 1st nodes in relation to experimental data validation. On the other hand, in the thermocouple locations 3, 4 and 5 were quite a bit diverged. Based on the phenomena, higher power is resulting with higher temperature results. Additionally, Table 11 shows the volumetric flow rate inside the system for each nominal power case and different power reduction cases.

39

Table 11. System flow rate results from power reduction analysis for valve 25% open case

Case	Volumetric Flow Rate (lpm)
Nominal Power	8.1513
90% Power	7.8356
80% Power	7.4979

According to the results, there is trend when the power was reduced by 10%, the volumetric flow rate was reducing by almost 4%. Thus, from this investigation, a hint was caught that with reducing the power at a certain rate, the results can be estimated. Also, the reason why there is not an investigation on reducing the power more than 20% of nominal power was that not to go more beyond the nominal power used in the system. Also, in this study, power increment sensitivity study was not investigated. As the model was prepared for both pressure drop cases with a different power levels as shown in Table 7, with the power that was used in the simulation for valve 100% open case was resulting with quite a bit higher temperature development than the experimental data. That's why, in this study, going beyond the power values that were used for simulation was not aimed for the sensitivity analysis.

6.5. Results from Accident Scenario (Two-phase Flow) Simulations

According to the nodalization diagram that described above (in Figure 11) the two-phase flow through valve 100% open case was simulated and analyzed. In addition to the steady-state simulation procedure, in the two-phase flow analysis simulation

duration time was raised to 43000 seconds so to see the temperature and system flow rate development inside the system. After reaching steady-state condition where the simulation time at 8000 seconds, the water supply from the cooling system was cut (components 700 and 750) at 8005 seconds. At the 43000 seconds, the simulation was cut due to similar behavior continuing. Through this simulation, boundary condition at component 770 was set at atmospheric pressure. As described in Figure 10, the system was left to form with the component 900 which is the water tank's rest empty part. From the procedure described, the cavity inlet, cavity outlet temperatures and system flow rate results were plotted and shown in Figure 22. Also, the computational results with experimental results that is published in [17] were compared. But through comparison in two-phase flow analysis, the priority was not aimed to validate the computational results against experimental results due to the different start-up procedure and initial conditions that had been followed. Based on the phenomena on the instabilities, results were analyzed in relation to the literature.
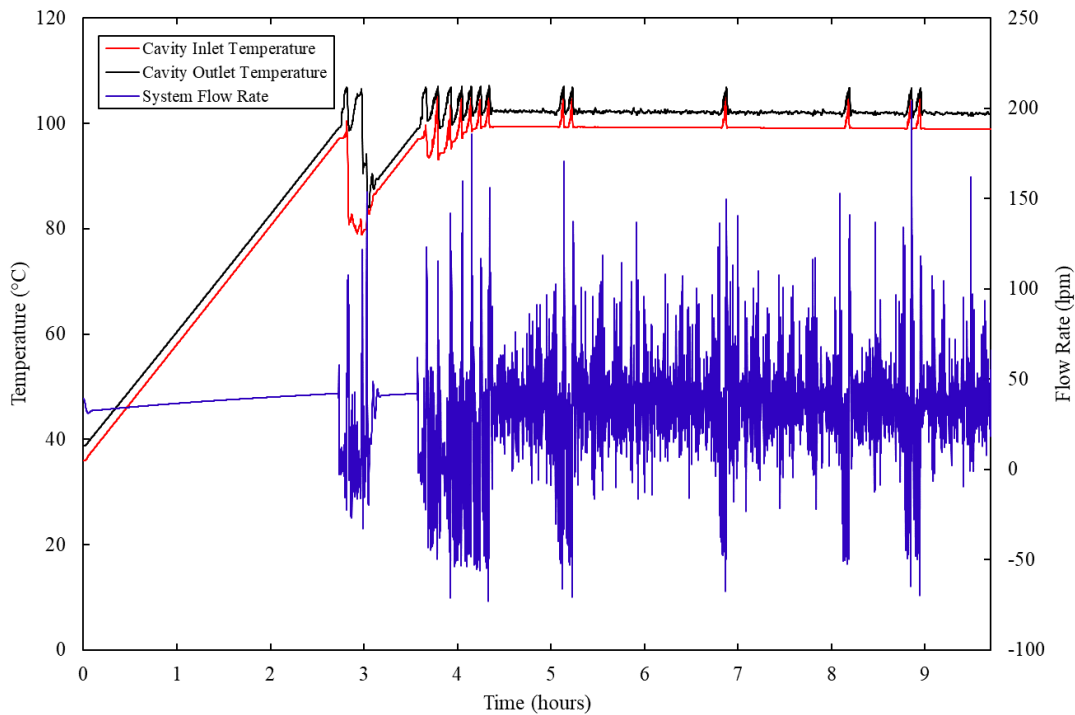
Figure 22. Two-phase flow analysis temperature and system flow rate results

The results were showing oscillatory behavior and cavity in and cavity out temperature values were superimposed for reference. In the Figure 22, the steady-state condition's results were trimmed and the time at 0, the system was developing by itself and the initial conditions for this two-phase flow analysis were cavity in and cavity out temperature values at 309°K and 312°K respectively and system flow rate at 39.06 lpm. From beginning to around 2.8 hours, the cavity in and cavity out temperature values were in steady increasing condition until saturation. In addition to the experimental limitations on the measuring the flow in a backward direction or beyond the certain limit due to the instrumentation, in simulation, there was a chance to see the flow even if it was occurring through backward direction. As the flow went below zero meaning with flowing in a backward direction, the system reacted with the instability. When system

42

showed first instability in system flow rate, the temperature results were at the saturation at a same time.

It was noted that the cavity in temperature was decreasing as system flow rate was decreasing. However, the cavity out temperature was behaving sharply increment as the flow was decreasing due to water flowing through heating section was decreasing. Then flow excursion was seen due to the saturation. After releasing the steam from the system for the first time, the flow followed with resumption of normal flow.

The normal flow continued around 28 minutes, then after the flow suddenly stopped again and the system behaved similar what happened before and at this time the instabilities were maintaining periodically for a while. After periodic instabilities, the system showed stable temperature results in cavity in and cavity out locations but oscillatory behavior in system flow rate. After the about 4.5 hours, instabilities were seen that were related to the flow going below zero for four times until the simulation finished.

The phenomena on the instabilities were analyzed and found similar behavior with geysering and flashing through literature in [14], [15]. Geysering was expected to occur in the heating section while the flashing was expected to occur in vertical section of the hot leg. Geysering phenomena is standing on, boiling initiates through the heating and bubbles are suddenly enlarged. That boiling condition gives a chance to be generated vapor and leaves the heating section in subcooled. In case of flashing, as the water leaves the heating section in subcooled, it rises through vertical section of the hot

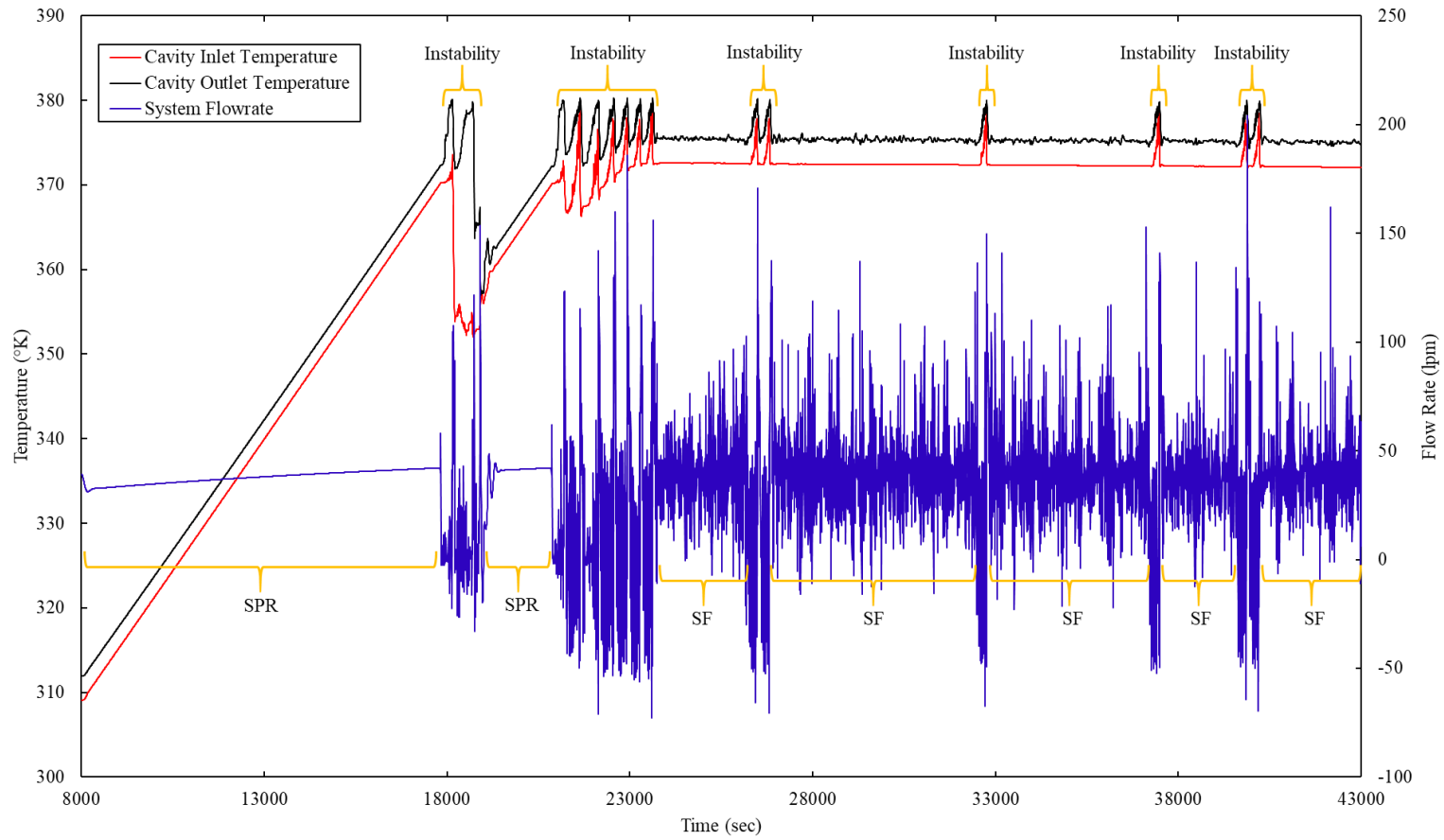leg and reaches saturation by depressurization and increases the system flow rate

sharply.

Figure 23. Flow classification in the two-phase flow analysis. Single phase region, and steady flashing regions are represented with SPR and SF respectively.

From the Figure 23, the flow was classified based on the phenomena that they had. For the first region that was single-phase region (SPR), the water temperature was developing by the heating. Then, the first instability was encountered due to saturation. Single-phase region follows and the next, periodic instabilities that were related to the geysering and flashing occurred. And steady flashing due to boiling in the hot leg all the rest of time. To analyze the instabilities easily, the results were divided in three different time scale.

In Figure 24, the first instability was analyzed and divided the time scale where the time was between 17500 seconds to 20000 seconds. In this figure, the system flow rate with blue line, saturation temperature value in the riser with orange line, 9 each riser's 6th node (riser's exit) water temperature values with five shades of grey, and the saturation temperature and water temperature in the hot leg vertical's exit with yellow and green respectively were illustrated.
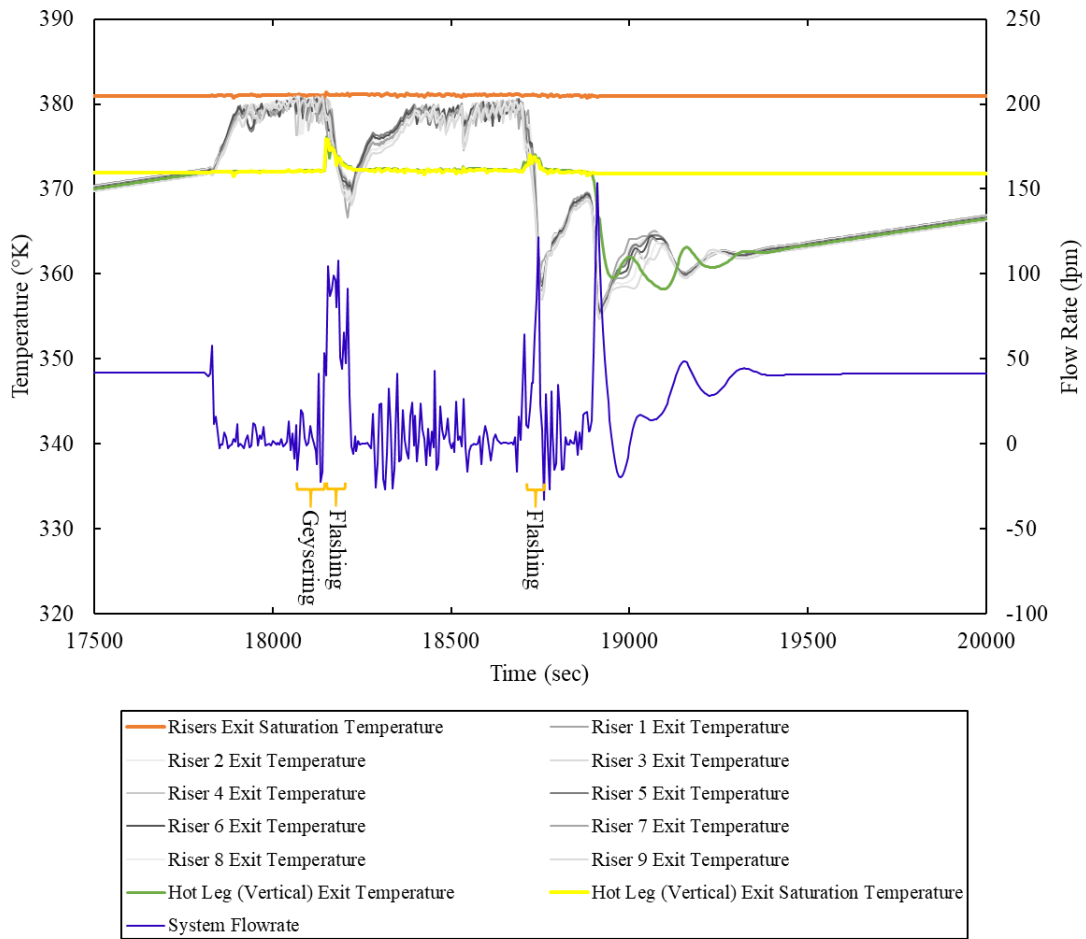
Figure 24. Two-phase flow analysis at the time between 17500 sec - 20000 sec

Three flashing events were seen in this time scale in Figure 24. While the system was behaving stable, at time 17830 sec the water in the risers reaches the subcooled and water in the hot leg vertical component's exit reaches saturation. From then, the flow went down sharply to zero for a while so to water in the risers development and saturation. When the water inside the risers reached the saturation (geysering), the water at the hot leg vertical component's exit reacted with flashing. And it can be seen that the system flow rate went up sharply when the flashing occurred at corresponding place and the water temperature in the risers went down. After flow rate excursion, same condition

47

repeated itself. But at the second time, the flashing occurred without geysering event due to water not reaching saturation in the risers. And the last flashing when at around 18900 sec occurred due to the water condensation in the hot leg's horizontal component at corresponding time. So that, at rest time period, system flow rate behaved stable, and the temperature results were stable increasing because of not facing saturation in any place.
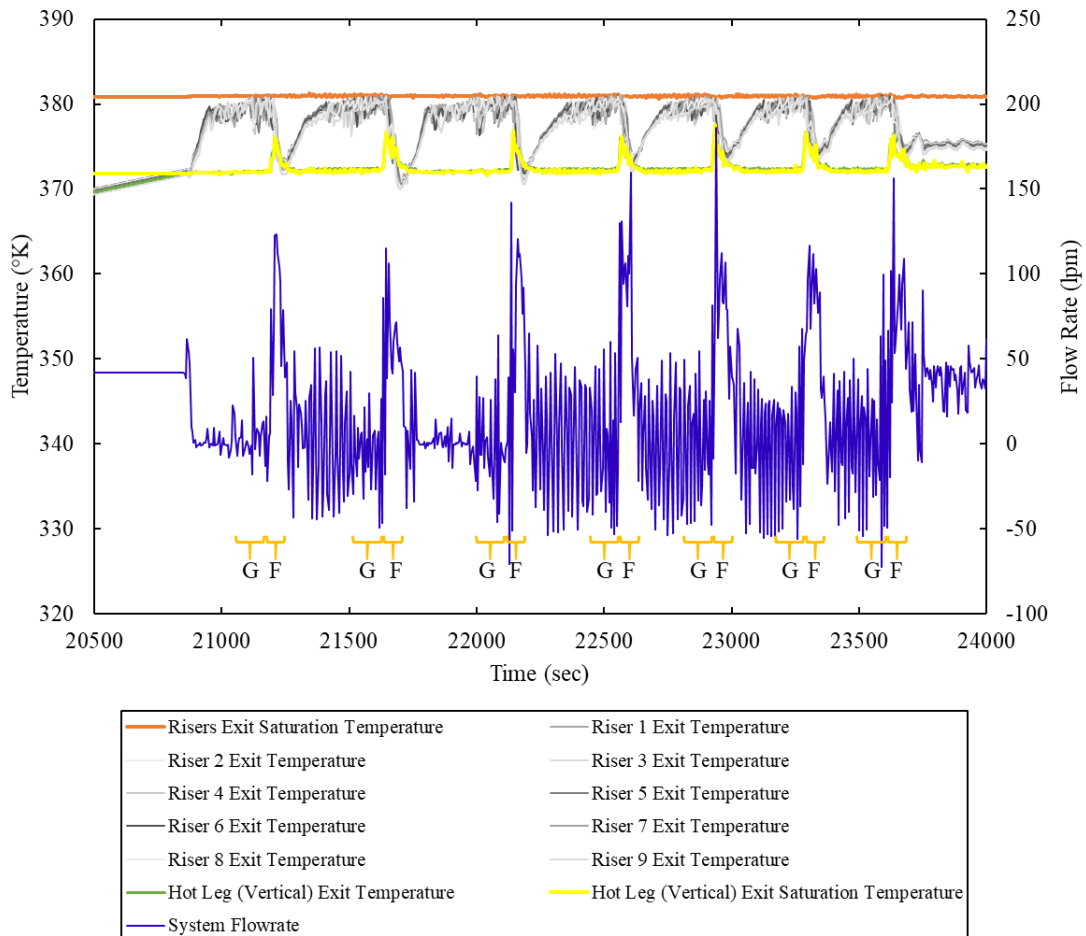

Figure 25. Two-phase flow analysis at the time between 20500 sec - 24000 sec

In addition to the previous classification, in Figure 25, the periodic flashing was seen through the time scale from 20500 sec to 24000 sec. In relation to the previous

analysis in Figure 24, in this analysis in Figure 25, there was similar behavior in the system. When the water saturated in the hot leg vertical component's exit, the flow went down to zero and helped to saturate water in the risers and finalized with geysering in risers' exit and flashing in the hot leg vertical component's exit. At this time scale, the period of flashing was about 6.8 mins.
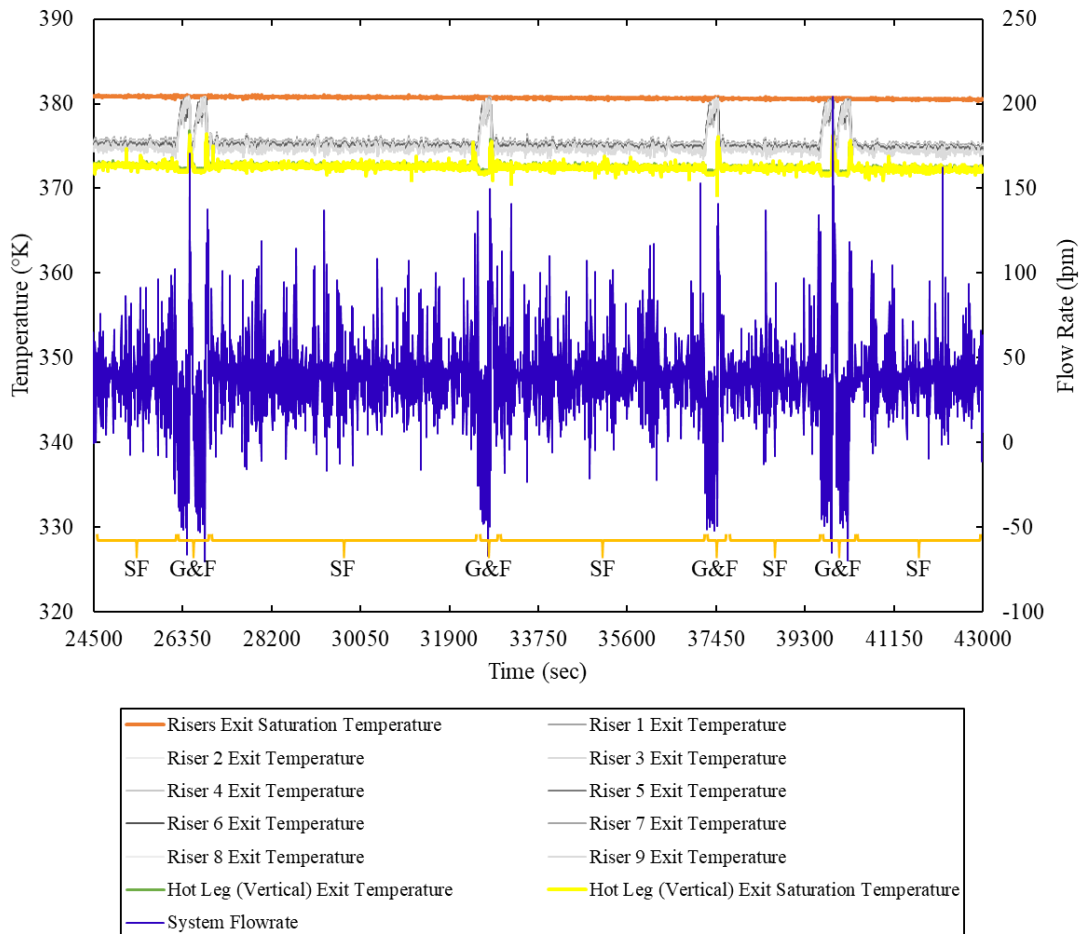

Figure 26. Two-phase flow analysis at the time between 24500 sec - 43000 sec

The last two-phase flow analysis in Figure 26, the model reacted with steady flashing, geysering and flashing behaviors. The system flow rate was oscillating due to the boiling in the hot leg vertical component's exit. In the steady flashing periods, the

risers' exit temperature values were way below from the saturation and remain steady until the saturation around 26000 sec to 27000 sec and so on. When the flow dipped and with backward flow, the model came up with the geysering and flashing.

Also, the simulation results were compared with the experimental results available through publication. Based on different start-up procedure and initial conditions, overall, the computational results were quite a bit different through comparison with experimental results. But some sort of behavior was still similar like cavity in and cavity out temperature development and values but that similarities happened in a different time.

7. CONCLUSION

In this study, the RELAP5/SCDAPSIM model that was built based on the small scaled (1/23) experimental facility used to investigate thermal hydraulic behavior of the RCCS experimental facility at Texas A&M University. After building the model, steady-state condition was simulated with different pressure drop cases inside the system which were valve 25% open case and valve 100% open case to validate the model against experimental data. After small modifications, the computational results for valve 25% open case were validated against experimental data and results for valve 100% open case had good agreement with experimental data.

Once satisfied with the computational results for steady-state condition, moved forward with sensitivity analysis that were flow splits in each riser, thermal stratification in upper manifold for both different pressure drop cases and power reduction study through valve 25% open case. From the results, hints caught on the flow splits and thermal stratification studies in relation to the heat distribution among the risers. For the power reduction study, focused on the understanding of the facility's response on different power values that were applied to the valve 25% open case's model.

The upgraded model for analyzing the two-phase flow was used to understand the flow characteristics, especially geysering and flashing phenomena, and system response during the accident conditions that involve the loss of the active heat removal. The flow instabilities were classified in relation to the literature.

For possible future study, uncertainty quantification of the model's parameters (i.e., power coefficients) could be important study to work.

REFERENCES

[1]   S. M. Goldberg and R. Rosner, "Nuclear Reactors: Generation to Generation," *Nucl. React.*, p. 40.

[2]   "Technology Roadmap Update for Generation IV Nuclear Energy Systems," p. 66.

[3]   H. S. Lim, N. Tak, S. N. Lee, and C. K. Jo, "Water-jacket reactor cavity cooling system concept to mitigate severe accident consequence of high temperature gas-cooled reactor," *Nucl. Eng. Des.*, vol. 340, pp. 156–165, Dec. 2018, doi: 10.1016/j.nucengdes.2018.09.029.

[4]   R. Vaghetto and Y. A. Hassan, "Experimental Investigation of a Scaled Water-Cooled Reactor Cavity Cooling System," *Nucl. Technol.*, vol. 187, no. 3, pp. 282–293, Sep. 2014, doi: 10.13182/NT13-130.

[5]   M. Corradini, M. Anderson, Y. Hassan, and A. Tokuhiro, "Experimental Studies of NGNP Reactor Cavity Cooling System With Water," NEUP--Project-09-781, 1063993, Jan. 2013. doi: 10.2172/1063993.

[6]   C. Tompkins and M. Corradini, "Flow pattern transition instabilities in a natural circulation cooling facility," *Nucl. Eng. Des.*, vol. 332, pp. 267–278, Jun. 2018, doi: 10.1016/j.nucengdes.2018.03.018.

[7]   L. Chen *et al.*, "Experimental verification on design model of the passive residual heat removal system of MHTGR," *Prog. Nucl. Energy*, vol. 98, pp. 23–28, Jul. 2017, doi: 10.1016/j.pnucene.2017.02.003.

[8]   D. D. Lisowski, T. C. Haskin, A. Tokuhiro, M. H. Anderson, and M. L. Corradini, "Study on the Behavior of an Asymmetrically Heated Reactor Cavity Cooling System with Water in Single," vol. 183, p. 14, 2013.

[9]   R. R. Schultz and H. Gougar, "Identification and Characterization of Thermal Fluid Phenomena Associated with Selected Operating/Accident Scenarios in Modular High Temperature Gas-cooled Reactors," p. 74.

[10]   S. J. Ball, "Next Generation Nuclear Plant Phenomena Identification and Ranking Tables (PIRTs) Volume 1: Main Report," ORNL/TM-2007/147, 1001275, Mar. 2008. doi: 10.2172/1001275.

[11]   N. R. Quintanar, T. Nguyen, R. Vaghetto, and Y. A. Hassan, "Natural circulation flow distribution within a multi-branch manifold," *Int. J. Heat Mass Transf.*, vol. 135, pp. 1–15, Jun. 2019, doi: 10.1016/j.ijheatmasstransfer.2019.01.102.

[12]   C. Tompkins and M. Corradini, "Flow pattern transition instabilities in a natural circulation cooling facility," *Nucl. Eng. Des.*, vol. 332, pp. 267–278, Jun. 2018, doi: 10.1016/j.nucengdes.2018.03.018.

[13]   D. D. Lisowski, O. Omotowa, M. A. Muci, A. Tokuhiro, M. H. Anderson, and M. L. Corradini, "Influences of boil-off on the behavior of a two-phase natural circulation loop," *Int. J. Multiph. Flow*, vol. 60, pp. 135–148, Apr. 2014, doi: 10.1016/j.ijmultiphaseflow.2013.12.005.

[14]   X. Yan, G. Fan, and Z. Sun, "Study on flow characteristics in an open two-phase natural circulation loop," *Ann. Nucl. Energy*, vol. 104, pp. 291–300, Jun. 2017, doi: 10.1016/j.anucene.2016.12.038.

[15]   X. Hou, Z. Sun, G. Fan, and L. Wang, "Experimental and analytical investigation on the flow characteristics in an open natural circulation system," *Appl. Therm. Eng.*, vol. 124, pp. 673–687, Sep. 2017, doi: 10.1016/j.applthermaleng.2017.05.201.

[16]   Q. Wang, P. Gao, X. Chen, Z. Wang, and Y. Huang, "An investigation on flashing-induced natural circulation instabilities based on RELAP5 code," *Ann. Nucl. Energy*, vol. 121, pp. 210–222, Nov. 2018, doi: 10.1016/j.anucene.2018.07.035.

[17]   R. Vaghetto and S. Yang, "Two-phase flow measurements and observations in a cooling panel of the reactor cavity cooling system," *Prog. Nucl. Energy*, vol. 131, p. 103578, Jan. 2021, doi: 10.1016/j.pnucene.2020.103578.

[18]   R. Vaghetto and Y. A. Hassan, "Modeling the thermal–hydraulic behavior of the reactor cavity cooling system using RELAP5-3D," *Ann. Nucl. Energy*, vol. 73, pp. 75–83, Nov. 2014, doi: 10.1016/j.anucene.2014.06.026.

[19]   C. M. Allison and J. K. Hohorst, "Role of RELAP/SCDAPSIM in Nuclear Safety," *Sci. Technol. Nucl. Install.*, vol. 2010, pp. 1–17, 2010, doi: 10.1155/2010/425658.

[20]   C. M. Allison, R. J. Wagner, L. J. Siefken, and J. K. Hohorst, "The Development of RELAP5/SCDAPSIM/MOD4.0 for Reactor System Analysis and Simulation," p. 1.